An Anti-Swing Controller for Aerial Transportation System with Flexible Suspending Rope

Zhaopeng Zhang
Institute of Robotics and Automatic Information System
College of Artificial Intelligence, Nankai University
Tianjin, China
zhangzp@mail.nankai.edu.cn

Xiao Liang
Institute of Robotics and Automatic Information System
College of Artificial Intelligence, Nankai University
Tianjin, China
liangx@nankai.edu.cn

Zhuang Zhang
Institute of Robotics and Automatic Information System
College of Artificial Intelligence, Nankai University
Tianjin, China
zhangzhuang@mail.nankai.edu.cn

Jianda Han
Institute of Robotics and Automatic Information System
College of Artificial Intelligence, Nankai University
Tianjin, China
hanjianda@nankai.edu.cn

Abstract—Numerous researches on aerial transportation uses the assumption that the payload is connected via a rigid rope. Although this assumption makes sense in most situations, it will still lose effectiveness occasionally. Therefore, this paper considers the dynamics and control of a system with flexible rope. Based on assumed mode method(AMM) and the assumption that the length of the rope remains unchanged, the dynamic model of this system is established by Euler-Lagrange techniques. Subsequently, through the energy-based analysis method, we design a nonlinear anti-swing controller. Asymptotic results are obtained with rigorous theoretical derivations provided by the Lyapunov-based stability analysis and LaSalle's invariance theorem. Two groups of simulation results are provided to demonstrate the superior performance of the proposed controller.

Index Terms—unmanned aerial vehicle(UAV), assumed mode method(AMM), anti-swing control, flexible transportation

I. INTRODUCTION

In recent years, with the continuous development of mechanical, electronic and material technologies, the utilization of quadrotor unmanned aerial vehicles(UAVs) has been greatly promoted, including military, aerial photography, pesticide spraying and so on. Due to the underactuation, nonlinearities and the coupling behaviour between quadrotor's outer loop and inner loop, the control problem of quadrotor UAVs is a challenging issue. Many researches propose numerous advanced methods [1]–[4] to deal with different control problems of quadrotors.

An important application field of quadrotor UAVs is transportation. There exists three main approaches, gripping by grippers [5], manipulation by robotic arm [6]–[8], and suspending by ropes [9]–[11]. In [5], by installing a gripper

beneath the UAV, quadrotor can transport various objects. The authors of [6] design a aerial manipulator with a 2-DOF robotic arm. Then, an autonomous flight experiment is conducted including picking up and delivering an object with a corresponding adaptive sliding mode controller. In [7], authors design a human-like dual arm aerial manipulator, which could be used in transportation. In [8], authors use model-based method to compensate the influence from robotic arm's motion. The designed controller achieves satisfactory performance and successfully completes grasping and transporting mission. However, the above methods are hard to transport large cargoes flexibly because of their very limited workspace. What's more, both a gripper and a robotic arm bring extra coupling, which increases the difficulty of accurate control. In conclusion, just in terms of transporting mission, suspending cargoes beneath the fuselage by a rope may be an ideal way for cargo delivery.

Similar as underactuated overhead cranes [12], [13], the quadrotor UAV transportation system is also underactuated. Considering that the payload motion is totally caused by the UAV's translation and cannot be controlled directly, it is a tough work to have quadrotor UAV reach a desired position or track a desired trajectory accurately with the payload swing being suppressed simultaneously. Up to now, researchers have done a great deal of work on the control issue of quadrotor UAV transportation. In [9], a nonlinear hierarchical control scheme is proposed for a quadrotor transportation system, whose closed-loop stability has been proven by the Lyapunov-based stability analysis and LaSalle's invariance theorem. Besides, the proposed control law presents high control precision and effective payload swing suppression by experimental verification. The authors of [10] propose an energy coupling control law, which ensures the equilibrium point's asymptotic stability by utilizing Lyapunov techniques and LaSalle's invariance theorem. Experimental results showed the superior performance, even in some adverse circumstances

including external disturbances and parameter uncertainties. [11] presents a pure proportional-inspired guidance law and custom path-following control method for the delivery mission of a slung payload, which enables the soft landing.

In many cases, the previous work make an assumption that the rope is inelastic and massless. In most cases, this assumption describes the transportation system accurately, but the flexibility of the rope may appear in the cases of high inertia ropes or large wind disturbance. There are very few researches on the control issue of aerial flexible transportation system. Farhad *et al* in [14], [15] model the payload as a system of serially-connected links and analyze its dynamics. Then, they utilize a geometric nonlinear controller on it and the overall closed-loop system is proven to be asymptotically stable. The proposed controller's performance is confirmed by some numerical examples and preliminary experimental results. Actually, this kind of analysis method is very similar to double-pendulum transporting problem [16]. In the mathematical models built in [16], the flexibility of a rope is depending on the number of virtual links. However, the difficulty of analysis increases with the number of imaginary links.

Consequently, this paper considers another analysis method for this kind of system with a flexible rope. Firstly, based on the assumed mode method(AMM), the dynamic model is built through the Lagrange's modeling techniques. Then, we design an energy-based controller, which can reach asymptotic stability by Lyapunov techniques and LaSalle's invariance theorem.

The rest of this paper is organized as follows. Section II introduces the total process of the model establishment, including the introduction of AMM, the energy analysis part and dimension reduction. Section III designs a nonlinear controller through energy-based method and gives the corresponding stability analysis. In Section IV, simulation tests are performed. Section V is a conclusion of the whole article.

II. Model Establishment

The schematic of an aerial transportation system with a flexible rope is shown in Fig. 1. Define $\boldsymbol{\xi}(t) = \left[y(t), z(t)\right]^{\top}$ as the position of the quadrotor UAV, θ as the roll angle of the quadrotor UAV. M and m represent the mass of UAV and the payload, respectively. ρ, l and S_0 represent the length, density and cross-sectional area of the flexible rope. Specially, x represents the distance between each point of the flexible rope to the tightened point in vertical direction, and x_e is the vertical distance of the rope's end point. Define $p(x,t)$ as the rope offset function of x and t. Define $\boldsymbol{q}_0 = \left[y, z, \phi, x_e\right]^{\top}$ as the state vector of the system.

It is assume that the rope length keep unchanged. That is

$$\chi = \int_0^{x_e} \sqrt{1 + \frac{\partial p(x,t)}{\partial x}} \mathrm{d}x - l = 0. \tag{1}$$

A. Energy Analysis

For the purpose of obtaining finite-dimensional dynamic model, this part firstly introduces AMM [17], [18], which is
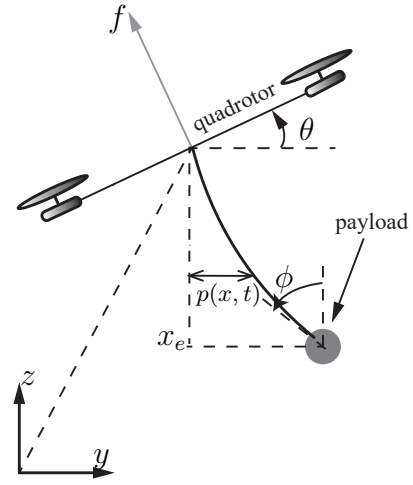
Fig. 1. Aerial transportation system with a flexible rope

a method using the linear sum of assumed modes to describe the vibration of an elastic body.

Assum $p(x,t)$ equals to a model function $\psi(x)$ timed by the mode state $\phi(t)$, which is

$$p(x,t) = \psi(x)\phi(t). \tag{2}$$

Then choose the following function to describe deformation of the rope:

$$\psi(x) = \cosh\left(\frac{\tau x}{l}\right) - \cos\left(\frac{\tau x}{l}\right) + \mu\left[\sin\left(\frac{\tau x}{l}\right) - \sinh\left(\frac{\tau x}{l}\right)\right], \tag{3}$$

where τ and μ and two positive constants.

Subsequently, Euler-Lagrange technique is applied to build up dynamics of the system. The kinetic energy includes three parts, including the motion of UAV, the oscillation of the payload and the swing of the rope as follows:

$$K = \frac{M}{2}(\dot{y}^2 + \dot{z}^2) + \frac{m}{2}[(\dot{y} + \psi(x_e)\dot{\phi})^2 + (\dot{z} - \dot{x}_e)^2]$$
$$+ \frac{\rho S_0}{2} \int_0^l [(\dot{y} + \psi(x)\dot{\phi})^2 + \dot{z}^2]dx. \tag{4}$$

As for the potential energy, the gravitational potential energy of UAV, the payload and the elastic potential energy of the rope are included as

$$P = Mgz + mg(z - x_e) + \frac{EJ}{2} \int_0^{x_e} \frac{(\psi''\phi)^2}{(1 + (\psi'\phi)^2)^3}dx, \tag{5}$$

where E and J are Young modulus and the rotational inertia.

Combining with the equation of invariable rope length (1), a constrained lagrangian is finally obtained,

$$L = K - P + \lambda\chi. \tag{6}$$

Taking (1), (4), (5) into (6) and substituting the result into Euler-Lagrange equation yields

$$\frac{\mathrm{d}}{\mathrm{d}t}\left(\frac{\partial L}{\partial \dot{\boldsymbol{q}}_0}\right) - \frac{\partial L}{\partial \boldsymbol{q}_0} = \boldsymbol{F}, \tag{7}$$

where $\boldsymbol{F}$ is the generalized force. Based on the above analysis, the dynamic equations of this aerial transportation system are derived as follows:

$$M_1\ddot{y} + M_2\ddot{\phi} + A_1\dot{x}_e\dot{\phi} = u_y, \tag{8}$$

$$M_1\ddot{z} - m\ddot{x}_e + G_1 = u_z, \tag{9}$$

$$m\ddot{x}_e - m\ddot{z} - A_1\dot{y}\dot{\phi} - \frac{1}{2}A_2\dot{\phi}^2 + G_2 - \lambda C_2 = 0, \tag{10}$$

$$M_3\ddot{\phi} + M_2\ddot{y} + A_1\dot{y}\dot{x}_e + A_2\dot{\phi}\dot{x}_e + G_3 - \lambda C_1 = 0, \tag{11}$$

where u_y, u_z stands for two control inputs, and

$$M_1 = M + m + \rho S_0 l, \quad M_2 = m\psi(x_e) + \rho S_0 \int_0^l \psi(x)dx,$$

$$M_3 = m\psi^2(x_e) + \rho S_0 \int_0^l \psi^2(x)dx,$$

$$G_1 = (M+m)g, \quad G_2 = \frac{EJ}{2}\frac{\phi\psi''(x_e)^2}{(1+(\phi\psi'(x_e))^2)^3} - mg,$$

$$G_3 = \phi EJ\left[\int_0^{x_e}\frac{\psi''^2 dx}{(1+(\phi\psi'')^2)^3} - 3\int_0^{x_e}\frac{(\psi'\psi'')^2 dx}{(1+(\phi\psi'')^2)^4}\right],$$

$$C_1 = \int_0^{x_e}\frac{\phi(\psi')^2}{\sqrt{(1+(\phi\psi')^2)}}dx, \quad C_2 = \sqrt{1+(\phi\psi(x_e))^2},$$

$$A_1 = m\psi'(x_e), \quad A_2 = 2m\psi(x_e)\psi'(x_e).$$

B. Reduce the Dimension of the System

Taking the time derivative of (1) yields

$$C_1(\phi, x_e)\dot{\phi} + C_2(\phi, x_e)\dot{x}_e = 0. \tag{12}$$

According to implicit function existence theorem, because C_2 is positive and bounded, system state x_e can be presented by ϕ. Therefore, by reducing dimensions of the system, a new form of dynamic model could be written as

$$M_1\ddot{y} + M_2(\hat{x}_e)\ddot{\phi} + A_n\dot{\phi}^2 = u_y, \tag{13}$$

$$M_1\ddot{z} + M_m\ddot{\phi} + A_m\dot{\phi}^2 + G_1 = u_z, \tag{14}$$

$$M_2(\hat{x}_e)\ddot{y} + M_m\ddot{z} + M_p\ddot{\phi} + A_p\dot{\phi}^2 + G_p = 0, \tag{15}$$

where

$$M_m = m\frac{C_1}{C_2}, \quad M_p = \left(M_3(\hat{x}_e) + m\frac{C_1^2}{C_2^2}\right),$$

$$G_p = \left(G_3(\hat{x}_e) - \frac{C_1}{C_2}G_2(\hat{x}_e)\right),$$

$$A_n = A_1(\hat{x}_e)\left(-\frac{C_1}{C_2}\right), \quad A_m = \frac{m}{C_2}\Gamma,$$

$$A_p = m\frac{C_1}{C_2^2}\Gamma - \frac{A_2(\hat{x}_e)}{2}\frac{C_1}{C_2},$$

$$\Gamma = \frac{\partial C_1}{\partial \phi} - \frac{C_1}{C_2}\left(\frac{\partial C_1}{\partial x_e} + \frac{\partial C_2}{\partial \phi}\right) + \frac{C_1^2}{C_2^2}\frac{\partial C_2}{\partial x_e}.$$

After rewritting the equation of dimension-reduced system dynamics, the state vector of the system becomes $\boldsymbol{q} = \left[\boldsymbol{\xi}^\top, \phi\right]^\top$. A compact form could be obtained as follows:

$$M_c(\boldsymbol{q})\ddot{\boldsymbol{q}} + V_c(\boldsymbol{q}, \dot{\boldsymbol{q}})\dot{\boldsymbol{q}} + G_c(\boldsymbol{q}) = U, \tag{16}$$

where

$$M_c(\boldsymbol{q}) = \begin{bmatrix} M_1 & 0 & M_2(\hat{x}_e) \\ 0 & M_1 & M_m \\ M_2(\hat{x}_e) & M_m & M_p \end{bmatrix},$$

$$V_c(\boldsymbol{q}, \dot{\boldsymbol{q}}) = \begin{bmatrix} 0 & 0 & A_n\dot{\phi} \\ 0 & 0 & A_m\dot{\phi} \\ 0 & 0 & A_p\dot{\phi} \end{bmatrix}, \quad G_c(\boldsymbol{q}) = \begin{bmatrix} 0 \\ G_1 \\ G_p \end{bmatrix}.$$

Two properties of the dynamic equation are given as follows:
Property 1: $\dot{M}_c(\dot{\boldsymbol{q}}) - 2V_c(\boldsymbol{q}, \dot{\boldsymbol{q}})$ is skew-symmetric.
Property 2: $M_2(\hat{x}_e)$ is positive and bounded.

III. CONTROLLER DEVELOPMENT AND STABILITY ANALYSIS

Let $\boldsymbol{\xi}_d = [y_d, z_d]^\top$ be the desired position of UAV. The control objective is to drive the quadrotor to the desired position, while eliminating the payload swing, which can be quantified as follows:

$$\lim_{t\to\infty}\boldsymbol{\xi}(t) = \boldsymbol{\xi}_d, \quad \lim_{t\to\infty}\phi(t) = 0.$$

To facilitate subsequent controller development and analysis, define the outer loop tracking errors $e_y(t) = y(t) - y_d$, $e_z(t) = z(t) - z_d$.

A. Controller Development

The total mechanical energy of the outer loop subsystem consists of both kinetic energy and potential energy as

$$E_m = \frac{1}{2}\dot{\boldsymbol{q}}^T M(\boldsymbol{q})\dot{\boldsymbol{q}} + \frac{EJ}{2}\int_0^{x_e}\frac{(\psi''\phi)^2}{(1+(\psi'\phi)^2)^3}dx + mg(l - x_e). \tag{17}$$

By using *Property 1*, taking the time derivative of E_m yields

$$\begin{aligned} \dot{E}_m &= \frac{1}{2}\dot{\boldsymbol{q}}^T \dot{M}(\boldsymbol{q})\dot{\boldsymbol{q}} + \dot{\boldsymbol{q}}^T M(\boldsymbol{q})\ddot{\boldsymbol{q}} + \dot{\boldsymbol{q}}^T\frac{\partial P}{\partial \boldsymbol{q}} \\ &= \frac{1}{2}\dot{\boldsymbol{q}}^T \dot{M}(\boldsymbol{q})\dot{\boldsymbol{q}} + \dot{\boldsymbol{q}}^T[U - G_c(\boldsymbol{q}) - V_c(\boldsymbol{q}, \dot{\boldsymbol{q}})\dot{\boldsymbol{q}}] + \dot{\phi}G_p \\ &= \dot{\boldsymbol{q}}^T U - \dot{z}(M+m)g \\ &= \dot{y}u_y + \dot{z}u_z - \dot{z}(M+m)g. \end{aligned} \tag{18}$$

Base on above analysis, choose a positive definite scalar function as the Lyapunov candidate function

$$V(t) = E_m + \frac{k_{py}}{2}e_y^2 + \frac{k_{pz}}{2}e_z^2. \tag{19}$$

Taking the time derivative of $V(t)$ leads to

$$\begin{aligned} \dot{V}(t) &= \dot{E}_m + k_{py}e_y\dot{e}_y + k_{pz}e_z\dot{e}_z \\ &= \dot{y}(u_y + k_{py}e_y) + \dot{z}[u_z + k_{pz}e_z - (M+m)g], \end{aligned} \tag{20}$$

with $k_{py}, k_{pz} \in \mathbb{R}^+$ being positive control gains. According to the form of (20), the control inputs are designed as follows:

$$u_y = -k_{py}e_y - k_{dy}\dot{e}_y - k_{\phi y}\phi^2\dot{y}, \tag{21}$$

$$u_z = -k_{pz}e_z - k_{dz}\dot{e}_z - k_{\phi z}\phi^2\dot{z} + (M+m)g, \tag{22}$$

where $k_{dy}, k_{\phi y}, k_{dz}, k_{\phi z}$ are all positive control gains.

B. Stability Analysis

Theorem 1: The proposed controller u_y and u_z guarantee that the quadrotor UAV is driven to the desired position while the payload swing is damped out in the sense that

$$\lim_{t\to\infty} [y, \dot{y}, z, \dot{z}, \phi, \dot{\phi}, p]^\top = [y_d, 0, z_d, 0, 0, 0, 0].^\top \quad (23)$$

Proof: $V(t)$ is a positive definite scalar function. Substituting the designed controller (21) and (22) into (20) yields

$$\begin{aligned}\dot{V}(t) &= \dot{y}(u_y + k_{py}e_y) + \dot{z}[u_z + k_{pz}e_z - (M+m)g], \\ &= \dot{y}(-k_{dy}\dot{e}_y - k_{\phi y}\phi^2\dot{y}) + \dot{z}(-k_{dz}\dot{e}_z - k_{\phi z}\phi^2\dot{z}), \\ &= -(k_{dy} + k_{\phi y}\phi^2)\dot{y}^2 - (k_{dz} + k_{\phi z}\phi^2)\dot{z}^2 \le 0. \quad (24)\end{aligned}$$

Therefore, the closed-loop system is Lyapunov stable at the equilibrium point. $V(t)$ is bounded because $V(t)$ is positive definite and $\dot{V}(t)$ is semi-negative definite. Based on the forms of $V(t)$ and $E_m(t)$, it is obviously seen that

$$\begin{aligned}E_m, e_y, e_z \in \mathcal{L}_\infty &\Rightarrow y, \dot{y}, z, \dot{z}, \phi, \dot{\phi} \in \mathcal{L}_\infty \\ &\Rightarrow u_y, u_z \in \mathcal{L}_\infty. \quad (25)\end{aligned}$$

Then, define an invariant set Φ as

$$S = \left\{ y, \dot{y}, z, \dot{z}, \phi, \dot{\phi}, p(x,t) \middle| \dot{V}(t) = 0 \right\}.$$

According to the form of $\dot{V}(t)$ in (24), one has that

$$\dot{y} = \dot{z} = 0, \quad \ddot{y} = \ddot{z} = 0, \quad \dot{e}_y = \dot{e}_z = 0. \quad (26)$$

in this invariant set. Next, substituting the proposed controller (21) and (22) into system dynamic model (13)–(15) leads to

$$M_2(\hat{x}_e)\ddot{\phi} + A_n\dot{\phi}^2 = -k_{py}e_y, \quad (27)$$

$$M_m\ddot{\phi} + A_m\dot{\phi}^2 = -k_{pz}e_z, \quad (28)$$

$$M_p\ddot{\phi} + A_p\dot{\phi}^2 = -G_p. \quad (29)$$

Because it has been illustrated that $\dot{M}_2(\hat{x}_e) = A_n\dot{\phi}$ in *Property 1*, equation (27) can be transformed into

$$\frac{d}{dt}\left(M_2(\hat{x}_e)\dot{\phi} \right) = -k_{py}e_y. \quad (30)$$

What's more, it is obvious that e_y keeps unchanged in this invariant set by observing (26). Assuming that $e_y = c_1$ with c_1 being a constant, integrating (30) leads to

$$M_2(\hat{x}_e)\dot{\phi} = -k_{py}c_1 t + c_2. \quad (31)$$

In this equation, c_2 is another constant.

According to *Property 2*, $M_2(\hat{x}_e)$ is positive and bounded. Besides, the boundness of ϕ is proven. It is easy to conclude that $c_1 = 0$, otherwise $-k_{py}c_1 t \to \infty$ with $t \to \infty$. Consequently, in invariant set S, $e_y = c_1 = 0$, which means that $y = y_d$. With the conclusion that $c_1 = 0$, equation (31) could be transformed into

$$M_2(\hat{x}_e)\dot{\phi} = c_2. \quad (32)$$

If $c_2 > 0$, $\dot{\phi}$ will be positive, which is to say that ϕ will keep increasing. It is contradictory to the conclusion in (25). For the same reason, c_2 couldn't be negative. In other word, $c_2 = 0$. Therefore, in invariant set S, $\dot{\phi} = 0$ and $\ddot{\phi} = 0$.

Taking these two equations $\dot{\phi} = 0$ and $\ddot{\phi} = 0$ into (28) and (29) leads to

$$e_z = 0, \quad z = z_d, \quad G_p = 0. \quad (33)$$

According to the form of G_p, ϕ and G_p share the same plus-minus sign, so $\phi = 0$ is the unique solution of $G_p = 0$. The rope offset function $p(x,t) = 0$ as well. As a result, S only contains the equilibrium point, i.e.

$$S = \left\{ y = y_d, \dot{y} = 0, z = z_d, \dot{z} = 0, \phi = 0, \dot{\phi} = 0, p(x,t) = 0 \right\}. \quad (34)$$

Eventually, based on the previous analysis, by invoking LaSalle's invariance theorem [19], the proof for the *Theorem 1* is completed. ∎

IV. SIMULATION RESULTS

This section will present simulation tests to evaluate the performance of the proposed anti-swing controller. Two groups of compared simulation results will be shown. The numerical simulation is implemented on MATLAB/Simulink.

The system parameters are set as:

$$\mu = 0.9049; \quad \tau = 1.1741; \quad E = 2 \text{ N/m}^2;$$
$$J = 0.0048 \text{ kg} \cdot \text{m}^2; \quad M = 1.7 \text{ kg}; \quad m = 0.7 \text{ kg};$$
$$l = 0.75 \text{ m}; \quad S_0 = 1.77^{-6} \text{ m}^2; \quad \rho = 1150 \text{ kg/m}^3.$$

A. Group 1

In this group of simulation, the initial position and desired position of the quadrotor are set as follows:

$$\begin{bmatrix} y_0 \\ z_0 \end{bmatrix} = \begin{bmatrix} 0 \text{ m} \\ 1 \text{ m} \end{bmatrix} \Rightarrow \begin{bmatrix} y_d \\ z_d \end{bmatrix} = \begin{bmatrix} 1 \text{ m} \\ 1.5 \text{ m} \end{bmatrix}.$$

The PD controller gains are set as follows:

$$k_{py} = 3.1, k_{dy} = 6, k_{pz} = 1.5, k_{dz} = 4.$$

And the proposed anti-swing controller gains are set as

$$k_{py} = 3.3, k_{dy} = 6, k_{\phi y} = 85, k_{pz} = 1.5, k_{dz} = 4, k_{\phi z} = 49.$$

The simulation results are provided in Figs. 2–5. Fig. 2 and Fig. 3 show the position $y(t)$, $z(t)$ of the quadrotor UAV, the swing angle $\phi(t)$ of the payload and the vertical distance $x_e(t)$ between payload and UAV driven by PD and proposed controllers, respectively. Fig. 4 and Fig. 5 show curves of control inputs. It is seen that the proposed method could drive the quadrotor to the desired position accurately and guarantee payload swing suppressed, whose maximal amplitude is half of the results driven by PD controller. The vertical distance $x_e(t)$ in Fig. 2 and Fig. 3 is calculated according to the payload swing angle ϕ, which has been stated in (12).
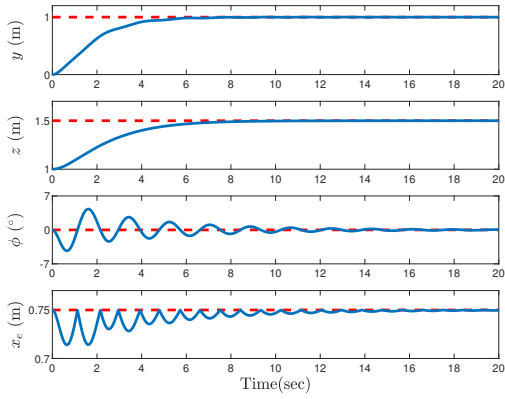
Fig. 2. Results for PD controller in *Group 1*: UAV position $y(t)$, $z(t)$, payload's swing angle $\phi(t)$ and the distance between payload and UAV in vertical direction $x_e(t)$
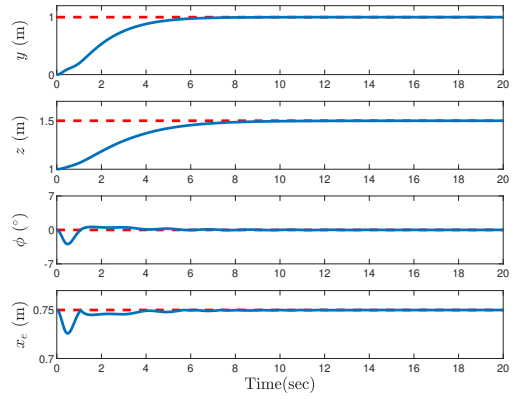
Fig. 3. Results for proposed controller in *Group 1*: UAV position $y(t)$, $z(t)$, payload's swing angle $\phi(t)$ and the distance between payload and UAV in vertical direction $x_e(t)$
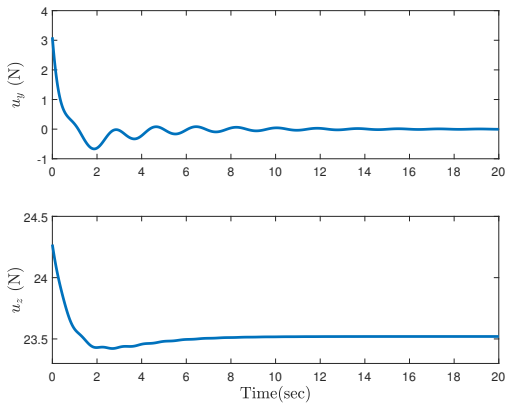
Fig. 4. Results for PD controller in *Group 1*: UAV's control inputs $u_y(t)$, $u_z(t)$
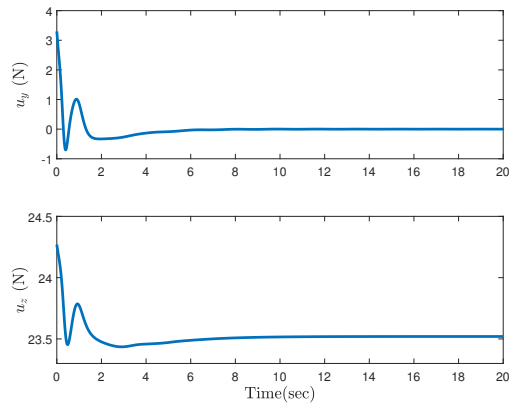
Fig. 5. Results for proposed controller in *Group 1*: UAV's control inputs $u_y(t)$, $u_z(t)$

B. Group 2

In this group of simulation, the initial position and desired position of the quadrotor are set as follows:

$$\begin{bmatrix} y_0 \\ z_0 \end{bmatrix} = \begin{bmatrix} 0 \text{ m} \\ 2 \text{ m} \end{bmatrix} \Rightarrow \begin{bmatrix} y_d \\ z_d \end{bmatrix} = \begin{bmatrix} 3 \text{ m} \\ 1 \text{ m} \end{bmatrix}.$$

The PD controller gains are set as follows:

$$k_{py} = 3.1, k_{dy} = 6, k_{pz} = 1.5, k_{dz} = 4.$$

And the proposed anti-swing controller gains are set as

$$k_{py} = 3.2, k_{dy} = 6, k_{\phi y} = 10, k_{pz} = 1.5, k_{dz} = 4, k_{\phi z} = 4.$$

Different from *Group 1*, this group simulates the situation of descending process rather than ascenting process. All the results are provided in Figs. 6–9. Due to the distance from the initial point to the desired point is farther than that of *Group 1* in horizontal direction, the resulting rope swing angle is larger than that of *Group 1*. It can be also seen that the proposed controller could suppress the payload swing more effectively.

V. CONCLUSION

By utilizing AMM, the swing motion of a flexible rope has been modeled as the form of a model function timed by a mode state, and then the dynamic model is built through the Euler-Lagrange's modeling techniques. Based on the resulting dynamic model, an energy-based controller is proposed, and the equilibrium point of the close-loop system is proven to be asymptotically stable by Lyapunov techniques and LaSalle's invariance theorem. According to two groups of simulation results, it can be validated that the proposed controller presents superior performance in suppressing the payload swing.

REFERENCES

[1] T. Lee, M. Leok and N. H. McClamroch, "Geometric tracking control of a quadrotor UAV on SE(3)," 49th IEEE Conference on Decision and Control, 2010, pp. 5420-5425.

[2] B. Zhao, B. Xian, Y. Zhang and X. Zhang, "Nonlinear Robust Adaptive Tracking Control of a Quadrotor UAV Via Immersion and Invariance Methodology," IEEE Transactions on Industrial Electronics, vol. 62, no. 5, pp. 2891-2902.

[3] Y. Choi and H. Ahn, "Nonlinear Control of Quadrotor for Point Tracking: Actual Implementation and Experimental Tests," IEEE/ASME Transactions on Mechatronics, vol. 20, no. 3, pp. 1179-1192.
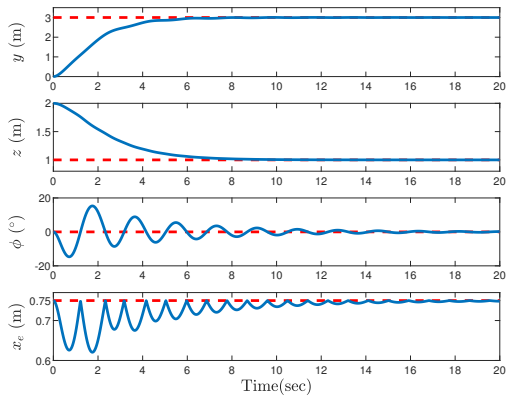
Fig. 6. Results for PD controller in *Group 2*: UAV position $y(t)$, $z(t)$, payload's swing angle $\phi(t)$ and the distance between payload and UAV in vertical direction $x_e(t)$
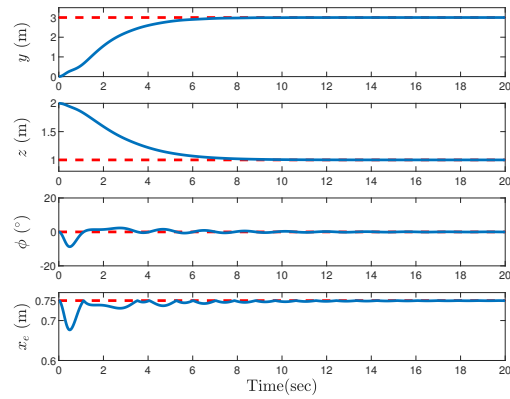
Fig. 7. Results for proposed controller in *Group 2*: UAV position $y(t)$, $z(t)$, payload's swing angle $\phi(t)$ and the distance between payload and UAV in vertical direction $x_e(t)$
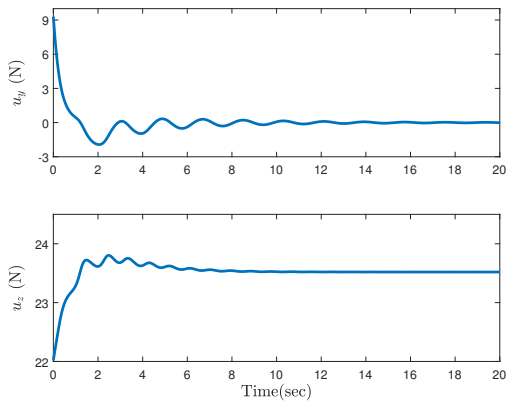
Fig. 8. Results for PD controller in *Group 2*: UAV's control inputs $u_y(t), u_z(t)$
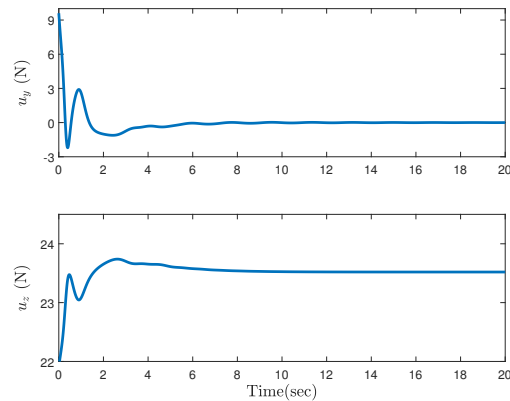
Fig. 9. Results for proposed controller in *Group 2*: UAV's control inputs $u_y(t), u_z(t)$

[4] F. Isabelle, R. Lozano and F. Kendoul, "Asymptotic stability of hierarchical inner-outer loop-based flight controllers," IFAC Proceedings, vol. 42, no. 2, pp. 1741-1746.

[5] D. Mellinger, Q. Lindsey, M. Shomin and V. Kumar, "Design, modeling, estimation and control for aerial grasping and manipulation," 2011 IEEE/RSJ International Conference on Intelligent Robots and Systems, 2011, pp. 2668-2673.

[6] S. Kim, S. Choi and H. J. Kim, "Aerial manipulation using a quadrotor with a two DOF robotic arm," 2013 IEEE/RSJ International Conference on Intelligent Robots and Systems, 2013, pp. 4990-4995.

[7] A. Suarez, F. Real, V. M. Vega, G. Heredia, A. Rodriguez-Castaño and A. Ollero, "Compliant Bimanual Aerial Manipulation: Standard and Long Reach Configurations," IEEE Access, vol. 8, pp. 88844-88865.

[8] G. Zhang, Y. He, B. Dai, F. Gu, J. Han and G. Liu, "Robust Control of an Aerial Manipulator Based on a Variable Inertia Parameters Model," IEEE Transactions on Industrial Electronics, vol. 67, no. 11, pp. 9515-9525.

[9] X. Liang, Y. Fang, N. Sun and H. Lin, "Nonlinear Hierarchical Control for Unmanned Quadrotor Transportation Systems," IEEE Transactions on Industrial Electronics, vol. 65, no. 4, pp. 3395-3405.

[10] X. Liang, Y. Fang, N. Sun and H. Lin, "A Novel Energy-Coupling-Based Hierarchical Control Approach for Unmanned Quadrotor Transportation Systems," IEEE/ASME Transactions on Mechatronics, vol. 24, no. 1, pp. 248-259.

[11] L. Qian, S. Graham and H. H.-T. Liu, "Guidance and Control Law Design for a Slung Payload in Autonomous Landing: A Drone Delivery Case Study," IEEE/ASME Transactions on Mechatronics, vol. 25, no. 4, pp. 1773-1782.

[12] N. Sun, Y. Fang and H. Chen, "A New Antiswing Control Method for Underactuated Cranes With Unmodeled Uncertainties: Theoretical Design and Hardware Experiments," IEEE Transactions on Industrial Electronics, vol. 62, no. 1, pp. 453-465.

[13] S. Ning, Y. Fang and X. Zhang, "Energy coupling output feedback control of 4-DOF underactuated cranes with saturated inputs," Automatica, vol. 49, no. 5, pp. 1318-1325.

[14] F. A. Goodarzi, D. Lee and T. Lee, "Geometric control of a quadrotor UAV transporting a payload connected via flexible cable," International Journal of Control, Automation and Systems, vol. 13, no. 6 pp. 1486-1498.

[15] F. A. Goodarzi, D. Lee, and T. Lee, "Geometric stabilization of a quadrotor UAV with a payload connected by flexible cable," 2014 American Control Conference, pp. 4925-4930.

[16] Y. Wu, N. Sun, X. Liang, Y. Fang and X. Xin, "A Robust Control Approach for Double-Pendulum Overhead Cranes With Unknown Disturbances," 2019 IEEE 4th International Conference on Advanced Robotics and Mechatronics, 2019, pp. 510-515.

[17] H. Gao and W. He, "Fuzzy control of a single-link flexible robotic manipulator using assumed mode method," 31st Youth Academic Annual Conference of Chinese Association of Automation, 2016, pp. 201-206.

[18] C. Sun, H. Gao, W. He and Y. Yu, "Fuzzy Neural Network Control of a Flexible Robotic Manipulator Using Assumed Mode Method," IEEE Transactions on Neural Networks and Learning Systems, vol. 29, no. 11, pp. 5214-5227.

[19] H. K. Khalil, Nonlinear systems. Upper Saddle River, NJ, USA: Prentice-Hall, 2002